

**GASIFICATION CHARACTERISTICS OF AN ACTIVATED CARBON
CATALYST DURING THE DECOMPOSITION OF HAZARDOUS WASTE MATERIAL
IN SUPERCRITICAL WATER**

Yukihiko Matsumura, Frederick W. Nuessle, and Michael J. Antal, Jr.

Hawaii Natural Energy Institute

University of Hawaii at Manoa, Honolulu, HI 96822

Key Words -- Carbon gasification, activated carbon, supercritical water

INTRODUCTION

Recently, carbonaceous materials including activated carbon were proven to be effective catalysts for hazardous waste gasification in supercritical water [1]. Using coconut shell activated carbon catalyst, complete decomposition of industrial organic wastes including methanol and acetic acid was achieved. During this process, the total mass of the activated carbon catalyst changes by two competing processes: a decrease in weight via gasification of the carbon by supercritical water, or an increase in weight by deposition of carbonaceous materials generated by incomplete gasification of the biomass feedstocks. The deposition of carbonaceous materials does not occur when complete gasification is realized. Gasification of the activated carbon in supercritical water is often favored, resulting in changes in the quality and quantity of the catalyst. To thoroughly understand the hazardous waste decomposition process, a more complete understanding of the behavior of activated carbon in pure supercritical water is needed.

The gasification rate of carbon by water vapor at subcritical pressures was studied in relation to both coal gasification and generating activated carbon [2]. It is known that carbon reacts with water vapor via:



A reaction mechanism which considers the competitive adsorption of water and hydrogen molecules to the same active sites was proposed [3-5]:



in which parentheses indicate the adsorbed species. Long and Sykes [5] assumed a steady state for the adsorbed molecules and succeeded in explaining results for subatmospheric conditions, using the rate equation:

$$r = \frac{k_1 p_{H_2O}}{1 + k_2 p_{H_2} + k_3 p_{H_2O}} \quad (6)$$

where k_1 , k_2 , and k_3 denote reaction rate constants, and p_{H_2O} and p_{H_2} are the partial pressure of water and hydrogen, respectively. This equation correctly predicts the inhibition by hydrogen observed in the experiment.

At elevated pressures, the generation of methane becomes more important. Gasification at steam pressures as high as 4.7 MPa was conducted by Blackwood and McGrory [6]. They proposed that the reaction between adsorbed hydrogen and water vapor for methane formation should be included with the reactions given by Eqs. 3 to 5, and correspondingly obtained the following rate equations:

$$r = \frac{k_1 p_{H_2O} + k_2 p_{H_2} p_{H_2O} + k_3 p_{H_2O}^2}{1 + k_2 p_{H_2} + k_3 p_{H_2O}} \quad (7)$$

$$r_{CH_4} = \frac{k_4}{k_4} p_{H_2O}, \quad (8)$$

where r_{CH_4} denotes the methane generation rate. These rate equations satisfactorily explained their results. Later, Van Heek et al. [7] found two mechanisms of methane generation: pyrolysis

coal at higher temperatures (higher than 600°C) for coal gasification in steam up to 7.1 MPa. Methane formation by pyrolysis was not intensified by pressure, but the rate of reaction between steam and char was clearly increased with pressure.

In spite of this accumulation of reaction data, we were unable to find measurements of the gasification rate of carbon in supercritical water. Data of this kind is needed to predict the lifetime of the catalyst and its contribution to the gas yields observed during biomass gasification. Consequently, the effects of temperature and pressure on the gasification rate and gas composition were measured and interpreted in relation to the previous research on carbon gasification under subcritical conditions. The change in iodine number of the carbon catalyst during supercritical water treatment was also measured.

EXPERIMENTAL

Experiments were conducted using a packed bed reactor [1] as shown in Fig. 1. The reactor was fabricated from Inconel 625 tubing, with a 9.53 mm OD and a 4.75 mm ID. Granular activated carbon (coconut shell based, 14-30 US mesh) was packed with a length of 406 mm in the reactor. Water was pressurized by an HPLC pump (Waters, Model 510) and fed to the reactor at 1.0 g/min. The temperature of the water flow was rapidly raised to the desired value by an entrance heater. The reactor was maintained at isothermal conditions by the furnace and a down-stream heater. The axial temperature profile along the reactor wall was measured using 11 type K thermocouples; another retractable type K thermocouple was placed inside the annulus of the reactor at the entrance of the packed bed. The pressure in the reactor system was measured by a pressure transducer. The reactor temperature was set at 600°C or 650°C, and the pressure was set at 25.5 MPa, 29.9 MPa, or 34.5 MPa.

After being cooled, the reactor effluent was sent to a sampling system principally composed of two three-way valves and a sampling loop. The effluent was discharged into the sampling loop for a defined duration, after which the contents were released into a pre-evacuated sampling tube. In the actual system, these two three-way valves were incorporated into one ten-port valve, enabling simultaneous switching of these valves. Effluent bypassing the sampling loop was delivered to an accumulator, where liquid and gas were separated and the gas was released through a pressure regulator, thus maintaining constant system pressure.

The gas generation rate was calculated from the pressure rise in the sampling tube, using the equation of state for an ideal gas. The change in gasification conversion with time was calculated using this measured gas generation rate and gas composition as determined by a gas chromatograph. Iodine tests (ASME D4607) were conducted to estimate the specific surface area of the residual carbons. BET surface area analysis was also conducted for a limited number of samples.

The iodine number of the virgin activated carbon was 1050. The ultimate analysis of this carbon showed the presence of hydrogen at 0.88 wt%.

RESULTS AND DISCUSSIONS

1. Total gasification rate

The composition of the product gas was similar for all the experimental conditions: hydrogen, 64%; carbon dioxide, 33%; methane, 2%; and carbon monoxide, 1% by mole. This composition was steady throughout the gasification. The ratio of hydrogen to carbon dioxide is close to 2, which is expected from the reactions shown in Eqs. 1 and 2.

It is known that the curves of carbon gasification conversion versus time can be often expressed by a single cubic equation in a normalized dimensionless plot using reduced time based on the time to attain a gasification conversion of 0.5 [8]. Although activated carbon is a partly gasified carbonaceous material, the normalized plot was drawn using conversion based on the initial activated carbon weight. In this work, the normalized plot was drawn using the reduced time τ based on the time needed for increasing conversion from 0.075 to 0.1 because the highest conversion was 0.25.

$$\tau = \frac{t - t_{0.075}}{t_{0.1} - t_{0.075}} \quad (9)$$

Here, t , $t_{0.075}$, and $t_{0.1}$ denote the time to be reduced, and times at which conversions of 0.075 and 0.1 were attained, respectively. The plots shown in Fig. 2 show good agreement for all the gasification experiments. This agreement indicates the possibility of using a single cubic equation to express the reaction rate change during gasification. It is also to be noted that the relation between conversion and reduced time is basically expressed by a linear function for the conversion range observed in this work.

From this graph of generalized conversion change, the dimensionless gasification rate at zero conversion is 0.0278. Dividing this value by the time needed to change conversion from

0.075 to 0.1 for each experiment gives the gasification rate at zero conversion for each experiment. These zero conversion values are used for the following data analysis, because they are not affected by the surface area change which occurs during gasification.

No clear trend with pressure was established, in agreement with the results from Long and Sykes [5]. (See Eq. 6, which shows that the effect of water vapor pressure becomes negligible at high pressures.) On the other hand, the earlier experiments by Blackwood and McGrory [6] predict a 20% increase in reaction rate with increasing pressure from 25.5 to 34.5 MPa at 600°C. Thus, the extrapolation of the results of Blackwood and McGrory [6] does not predict the effect of pressure within this pressure range.

The effect of temperature is shown in Fig. 3 in the form of an Arrhenius plot. Carbon gasification rates at 34.5 MPa, projected using the rate equations of earlier workers, are also shown in the figure. Extrapolation of the results from Long and Sykes [5] predicts our result accurately. From the results of our work, the activation energy was found to be 166 kJ/mol, which is in good agreement with 176 kJ/mol observed by Long and Sykes [5]. This agreement suggests that the fundamental mechanism of gasification does not change under high pressures such as the supercritical condition. The prediction using the rate equation by Blackwood and McGrory [6] presents a quite different dependence of the reaction rate on temperature.

2. Methane generation rate

No clear dependence of the methane generation rate on total pressure is observed, which suggests that methane generation occurs by pyrolysis [7]. The ratio of the methane generation rate to the total gasification rate is thus constant, showing a value around 3%. Assuming that all hydrogen in the original activated carbon turns into methane by pyrolysis, the ratio should be 2.8%, in agreement with the observed value. The prediction of this value using the rate coefficients determined by Blackwood and McGrory [6] gives 0.03%, which indicates reaction of steam with carbon at this temperature is very slow. Thus, it should be concluded that the methane generation observed here is due to pyrolysis of activated carbon.

3. Iodine number

The iodine number is a crude measure of the surface area of an activated carbon, obtained by analyzing its capacity for iodine adsorption. The relation between the iodine number and the conversion (see Fig. 4) shows at first an increase in the iodine number with increasing conversion, then maximum iodine number from 0.05 to 0.2, and finally a decrease in the iodine number at conversions above 0.2. The early increase in the iodine number is because of gasification accompanied with the development of the microporous structure. In the middle flat region, the microporous structure is maximized, and there is an equilibrium between creation of new pores and destruction of the walls between them. The decrease at high conversion indicates when the burn-off of the walls between the pores dominates over creation of new pores. Thus, short-term treatment in supercritical water effectively develops the microporous structure of the carbon. BET analysis showed a similar increase in surface area from 809 m²/g to 1011 m²/g after 6-hour reaction in supercritical water at 600°C and 34.5 MPa. No significant influence of pressure on the iodine number after a 6-hour treatment was observed.

4. Activated carbon production in supercritical water

This increase in the iodine number of carbon by treatment in supercritical water can be utilized for activated carbon production. A series of experiments were conducted to activate charcoals in supercritical water. Charcoals produced in-house (14-30 US mesh) were packed in the reactor in place of activated carbon, and after treatment in supercritical water at 600°C, 34.5 MPa, the iodine numbers of the product activated carbon were measured. Table 1 shows the results of these iodine tests. Large increases in the iodine number from the initial values of less than 50 are observed for each treatment. Thus, treatment of carbonaceous materials in supercritical water can be a novel approach for producing activated carbon production at lower temperatures than conventional activation methods.

CONCLUSION

The gasification rate of activated carbon in supercritical water is unaffected by variations in total pressure above the critical pressure of water, and is predictable by previous gasification measurements made at subatmospheric pressure, indicating the same gasification reaction mechanism. The methane generation characteristics indicate that methane is produced by the pyrolysis of the activated carbon itself. Short-term gasification in supercritical water increases the specific surface area of activated carbon, and thus its adsorbent capabilities. Supercritical water treatment can be a novel technique of activated carbon production at lower temperature than conventional activation methods.

Acknowledgment— This research was funded by DOE (DE-FC36-94AL 85804).

REFERENCES

1. X. Xu, Y. Matsumura, and M. J. Antal, Jr., submitted to *Ind. Eng. Chem. Res.* (1995).
2. J. L. Johnson, in *Chemistry of coal utilization, 2nd suppl. volume* (Edited by M. A. Elliot) p.1491. John Wiley & Sons, Inc., New York (1981).
3. J. Gadsby, C. N. Hinshelwood, and K. W. Sykes, *Proc. R. Soc. (London)*, **A187**, 129 (1946).
4. R. F. Strickland-Constable and D. Phil, *Proc. R. Soc. (London)*, **A189**, 1 (1947).
5. F. J. Long and K. W. Sykes, *Proc. R. Soc. (London)*, **A193**, 377 (1948).
6. J. D. Blackwood, and F. McGrory, *Aust. J. Chem.*, **11**, 16 (1958).
7. K. H. Van Heek, H. Juntgen, and W. Peters, *J. Institute Fuel*, **46**, 249 (1973).
8. P. L. Walker, Jr., in *Fundamentals of Thermochemical Biomass Conversion* (Edited by R. P. Pverand, T. A. Milne, L. K. Mudge) p.485. Elsevier, London (1985).

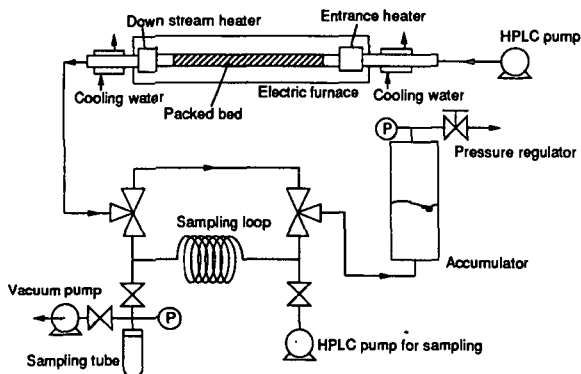


Fig. 1. Supercritical flow reactor scheme

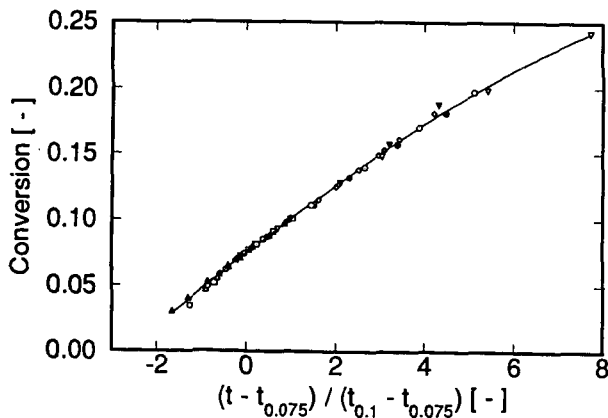


Fig. 2. Normalized plot for the gasification of activated carbon in supercritical water

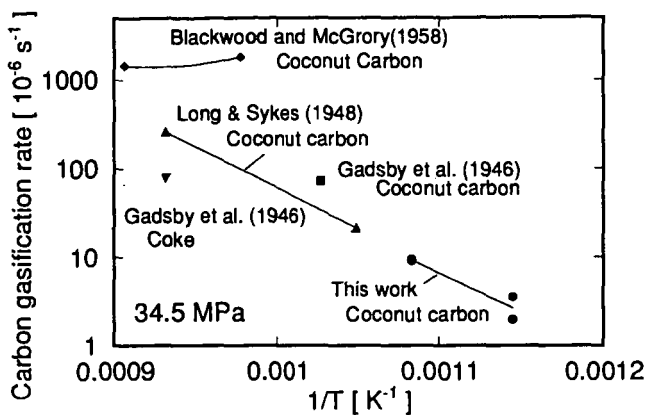


Fig. 3. Arrhenius plot for the gasification rate of carbon in water at 34.5 MPa

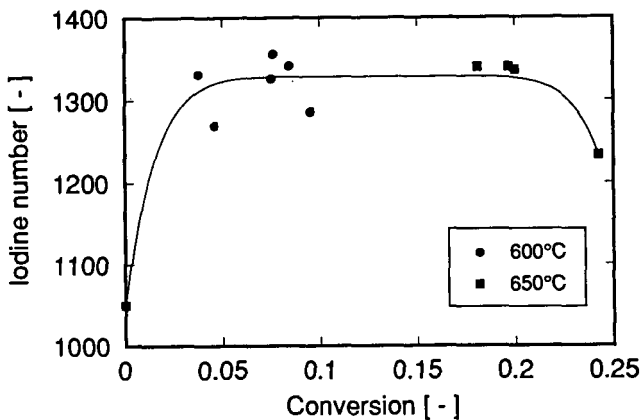


Fig. 4. Relationship between conversion and iodine number

Table 1. Increase in iodine numbers after treatment of charcoal in supercritical water at 600°C, 34.5 MPa.

Charcoal	Time [h]	Iodine number [-]	Conversion [-]
Macadamia nut shell	2	498	0.47
Macadamia nut shell	6	622	0.68
Macadamia nut shell (650°C)	6	689	0.49
Coconut husk	6	512	0.42
Coconut shell	6	450	0.22